IEEE Access
Multidisciplinary | Rapid Review | Open Access Journal

Received December 9, 2019, accepted January 1, 2020, date of publication January 13, 2020, date of current version January 23, 2020.

Digital Object Identifier 10.1109/ACCESS.2020.2966125

Compact Metamaterial Based 4 × 4 Butler Matrix With Improved Bandwidth for 5G Applications

ARSHAD KARIMBU VALLAPPIL[1], MOHAMAD KAMAL A. RAHIM[1], (Senior Member, IEEE), BILAL A. KHAWAJA[2,3], (Senior Member, IEEE), AND MUHAMMAD NAEEM IQBAL[1]

[1]Advance RF and Microwave Research Group (ARFMRG), Faculty of Engineering, School of Electrical Engineering, Universiti Teknologi Malaysia (UTM), Johor Bahru 81310, Malaysia
[2]Department of Electrical Engineering, Faculty of Engineering, Islamic University of Madinah, Madinah 41411, Saudi Arabia
[3]Department of Electronics and Power Engineering (EPE), PN-Engineering College (PNEC), National University of Sciences and Technology (NUST), Karachi 75104, Pakistan

Corresponding authors: Arshad Karimbu Vallappil (kvarshad2@graduate.utm.my) and Bilal A. Khawaja (7166@iu.edu.sa)

This work was supported in part by the Ministry of Education (MOE), in part by the Research Management Centre (RMC), School of Postgraduate Studies (SPS), and in part by the School of Electrical Engineering, Universiti Teknologi Malaysia (UTM), Johor Bahru, under Grant 04G65 and Grant 06G20.

ABSTRACT This paper proposes a novel compact 4 × 4 butler matrix (BM) with improved bandwidth based on open-circuit coupled-lines and interdigital capacitor unit-cell to develop composite right/left handed (CRLH) transmission-line (TL) metamaterial structure. The BM is implemented by the combination of compact 3dB quadrature hybrid couplers, 0dB crossover and 45° phase shifter on a single FR4 substrate ($\varepsilon_r = 4.3$ and $h = 1.66$ mm). The simulated and measured result shows that the return loss and isolation loss are better than 14 dB at all the ports, good insertion loss of -7 ± 2dB, which cover the frequency range of 3.2 GHz to 3.75 GHz. The phase difference of −45°, 135°, −135° and +45° are achieved with a maximum average phase tolerance of 5°. The overall dimension of the BM is 70mm × 73.7mm, which shows the compactness of the proposed design that is 75% size reduction and 8.2 times improvement in the bandwidth (550MHz) as compared to conventional BM. The CST microwave studio is used to design and perform the simulations. Additionally, the simulated and measured scattering parameters and phase differences show that they are in good agreement. This compact and improved bandwidth of the proposed BM is suitable for 5G antenna array beamforming network.

INDEX TERMS 5G, composite right/left handed (CRLH) transmission-line, metamaterial, beamforming network (BFN), Butler matrix (BM), branch line coupler (BLC).

I. INTRODUCTION

The evolution in wireless communication systems in terms of enhanced performance by improving data-rate, power dissipation and latency leads to the emergence of 5G [1], [2]. It is predicted that upcoming 5G technology will provide the end-users; data-rates of ∼10 GB/s (optical fibre-like experience), reduced end-to-end latency and improved capacity of up to several billion users as compared to the previous wireless systems [3]–[5]. Another significant feature of the planned 5G technology is to exploit microwave (around 3-6 GHz) as well as millimetre-wave (mm-wave) frequency bands [2], [5]. This leads to greater spectral bandwidths and directional antenna arrays which can transmit focus radiated power in any desired direction by using beamforming networks (BFNs) [5]. In addition to the smartphones, tablets and laptop computers, the huge influx of compact wireless-enabled wearable devices leads to an exponential increase in the wireless end-users who demand constant anytime, anywhere connectivity [6]. To provide good quality of service (QoS) with constant connectivity, the researchers have put a lot of efforts in the area of phased array antennas and their respective BFNs.

It is envisioned that in the upcoming 5G systems, phased array antennas (PAAs) will be playing a crucial role to get the desired output at the transceivers [7], [8]. The PAA consists of a BFN and antenna array. The main beam of an antenna is steered by the BFN network with the given phase and amplitude. There are many different types of BFNs reported in the literature [9]–[14], [16]–[18], [22]–[27]. The BFNs have two

The associate editor coordinating the review of this manuscript and approving it for publication was Qammer Hussain Abbasi.

categories 1) Rotman lens and 2) Circuit-based beamformer. The Rotman lens [14] provide wideband characteristics, but due to its extremely large size, it is not considered a promising candidate for 5G applications. The circuit based beamformers are further classified into three types, which are Nolen, Blass and Butler Matrix, respectively. The most commonly used BFN due to its easy fabrication process and low-cost is the butler matrix (BM) which is used for the antenna array feed. It requires N input ports (N beams), N output ports, ($N/2$) $\log_2(N)$ hybrid couplers, and ($N/2$) $\log_2(N-1)$ fixed phase shifters to form the $N \times N$ network [9]. Typical design of BM is a bilateral structure, which consists of three main components, i.e. couplers, crossovers and phase shifters.

The issue with conventional BM is that it has limited bandwidth and large size due to the hybrid couplers and phase shifters. So, the researcher started to introduce new designs of BM with an open-stub, modified hybrid branch line coupler (BLC), without crossover, without phase shifter and metamaterial transmission to minimize the size [10]–[15]. In [10], a miniaturized BM network implemented with the stub-loaded transmission lines is proposed and experimentally verified for multi-beam antenna array system. The size of the BM is reduced by 55% as compared to the conventional BM design. Another miniaturized BM design is presented in [12] by employing dumbbell-shaped cross-slot patch hybrid couplers and meandered lines based crossover. It achieves the fractional bandwidth improvement of 37.5% and a size reduction of 17%.

In [16], it is shown that the use of 45° and 90° phase shifters and four BLCs miniaturized by employing open-stubs in each transmission-line allows the size reduction of 42.68% as compared to the conventional BM. In [11], a miniaturized BM using cross-slot patch hybrid couplers and 45° phase shifters using short-circuited stubs are presented. The bandwidth of the BM is improved by 14%, and the size is reduced by 56% as compared to conventional BM, respectively. A novel compact BM without phase shifter is presented in [17] that contains couplers with −45° and −90° phase difference and a crossover. In [18], a novel electromagnetic metamaterial transmission-line (EM-MTM TL) is proposed by using the structure of symmetric double spiral lines (SDSLs). As per the literature review presented here, most of the discussed designs demonstrate a reduction in the area without much improvement in the bandwidth of the BM.

Therefore, in this paper, a compact and improved bandwidth BM is proposed by employing four 3dB BLCs based on the open-circuit coupled-lines technique and interdigital capacitor (IDC) CRLH-TL metamaterial structure [21], one 0dB crossover (instead of two 0 dB crossover in the conventional BM) and phase shifters of 45°. The crossover is designed by cascading two 3dB BLCs. The proposed 4 × 4 BM is designed by using the CST microwave studio software for 5G applications. The proposed BM is designed using the flame-resistant (FR4) copper-clad substrate [19] with relative permittivity (ε_r) dielectric constant of 4.3 and thickness of 1.66 mm. The simulation and measured results

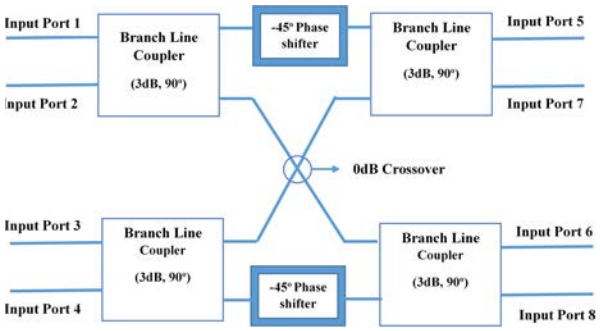

FIGURE 1. Block diagram showing the design of the proposed BM.

TABLE 1. Phase relation between ports at output of BM feed.

	Input Port 1	Input Port 2	Input Port 3	Input Port 4
Output Port 5	135^0	45^0	90^0	0^0
Output Port 6	90^0	180^0	-45^0	45^0
Output Port 7	45^0	-45^0	180^0	90^0
Output Port 8	0^0	90^0	-45^0	135^0
Phase Difference Between Consecutive Output Ports	-45^0	$+135^0$	-135^0	$+45^0$

suggest that the designed BM achieves excellent performance and it can be used as an ideal candidate for the beamforming network in the upcoming 5G antenna array systems.

The rest of the paper is organized as follows: Section 2 discusses the design configuration of the proposed BM and its relevant simulation and measured results. Section 3 presents the comparison of proposed work with the existing design, and finally, Section 4 draws conclusion.

II. BUTLER MATRIX DESIGN CONFIGURATION

The proposed BM comprises of four 90°BLCs, one crossover and two phase shifters which generate −45° phase shift. As shown in Fig. 1, it has four input ports labelled as port 1, port 2, port 3, and port 4 and four output ports labelled as port 5, port 6, port 7, and port 8, respectively.

Table 1 shows the phases that will be generated on each output port based on the selection of the input port. It has four cases; the phase difference between the consecutive output ports will be −45° when the input port 1 is excited. When the input port 2 is excited, the phase difference between the consecutive output ports will be 135°. For the third case, the phase difference between the consecutive output ports will be −135°, when the input port 3 is excited. When the input port 4 is excited, the phase difference between the output ports will be 45°.

The TL width and length of the BM element is calculated using microstrip feedline method [20], CST Microwave Studio software is used to perform all the design simulation and optimization of the individual components and also the

TABLE 2. Design specifications.

Parameters	Coupler	Crossover	Butler Matrix
Operating Frequency	3.5GHz	3.5GHz	3.5GHz
Method	Metamaterial transmission line	Metamaterial transmission line	Metamaterial transmission line
Required BW	1GHz	1GHz	500MHz
Phase Difference	90^0	0^0	$-45^0, 135^0, -135^0$,45^0
Insertion Loss	-3dB±2	0dB	-7±2dB
Return loss	Below -10dB	Below -10dB	Below -10dB
Isolation loss	Below -10dB	Below -10dB	Below -10dB

combination of coupler and crossover to construct the BM. The proposed BLC, crossover and BM were validated with the design specifications provided in Table 2. The detailed explanation and design of BM components are given below.

A. BRANCH LINE COUPLER (BLC)

The BLC used in this work is a compact design based on the CRLH-TL metamaterial structure. The CRLH-TL metamaterial structure is achieved by inserting the open-circuit coupled-lines and interdigital capacitor (IDC) unit-cell for the vertical and horizontal arm of the BLC as shown in Fig. 2 (a-b). The impedance of the horizontal and vertical arms TL of the BLC is 35Ω and 50Ω, respectively. The width and length of both the arms of the BLC can be calculated by using the formula [20], [21] based on the impedances mentioned above. The optimized dimensions of the IDC-CRLH unit-cell finger width (w_c), length (l_c) and gap (S) between the fingers are calculated and found to be 0.4mm, 3.9mm and 0.4mm, respectively based on Eq. (1-2) [22], [23]:

$$w_c \approx \frac{w}{\left(\frac{5N}{3} - \frac{2}{3}\right)} \tag{1}$$

$$s = \frac{2w_c}{3} \tag{2}$$

where in eq. (1), N indicates the number of fingers and $w = 5$mm refers to the width required to obtain the horizontal arm impedance of 35Ω. The dimension of the horizontal and vertical arm IDC unit-cell finger length l_c is optimized to be 3.9mm and 2.2mm, respectively for achieving the BLC center frequency of 3.5GHz. The horizontal and vertical IDC unit-cell finger length has a different dimension due to the impedance matching [20]. The open-circuit coupled-line inner strip width is 0.4mm. The IDC unit-cell and the fabricated BLC prototype are shown in Fig. 2(a-b), respectively. The BLC is considered as an important component for the BM design. The simulated and measured scattering parameter and phase difference results for the proposed BLC are

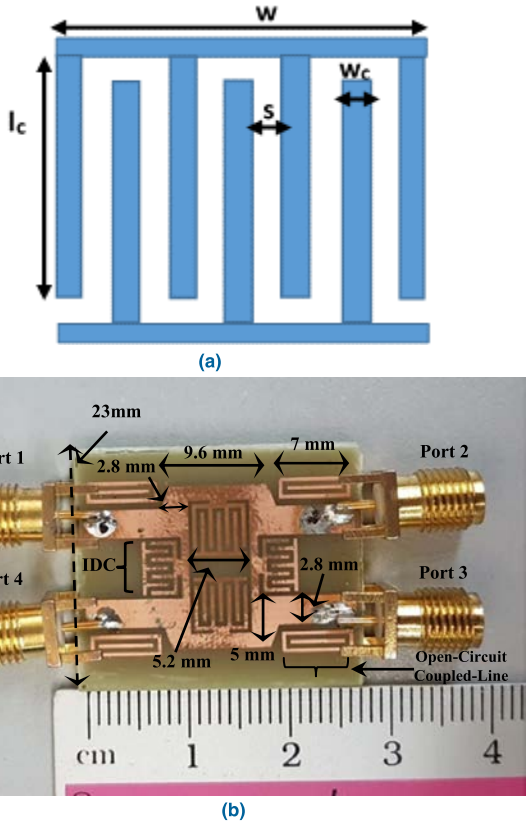

FIGURE 2. (a) IDC unit-cell (b) Fabricated prototype of the proposed BLC using FR4 substrate showing the respective BLC Ports 1-4, respectively and the PCB dimensions.

summarized in Fig. 3(a-b). The fabricated coupler operates between 2.74 GHz to 4.15 GHz frequency band for the return loss and isolation loss of below -10dB. The insertion loss result also shows very good performance and a variation of 3 ± 0.2dB in the same frequency band. The measured phase difference between the output ports is found to be 88°. The *λ/4* open-circuit coupled-lines and the IDC unit-cell are used to provide wide bandwidth and size reduction in the circuit.

B. 0dB CROSSOVER

The 0dB crossover is a four-port network with two input ports and two output ports named as port 1, port 4 and port 2, port 3, respectively. The crossover is designed by using two separate techniques. The first design consists of cascading two 3dB BLC combined together by using the copper tape and the glue, as shown in Fig. 4(a). It can be seen from Fig. 4(a) that in this design, both BLC shares the same ground plane, and it has an overall area of 59mm × 23mm, respectively. The second design of the crossover is considered compact because it is fabricated using single FR4 PCB with an overall area of 36mm x 23mm, as shown in Fig. 4(b). The total area of the compact crossover design shown in Fig. 4(b) is reduced by 39% as compared to the first design shown in Fig. 4(a). Since, the insertion loss S_{31} and S_{24} and the phase difference between S_{31} and S_{24} introduced by the two designs

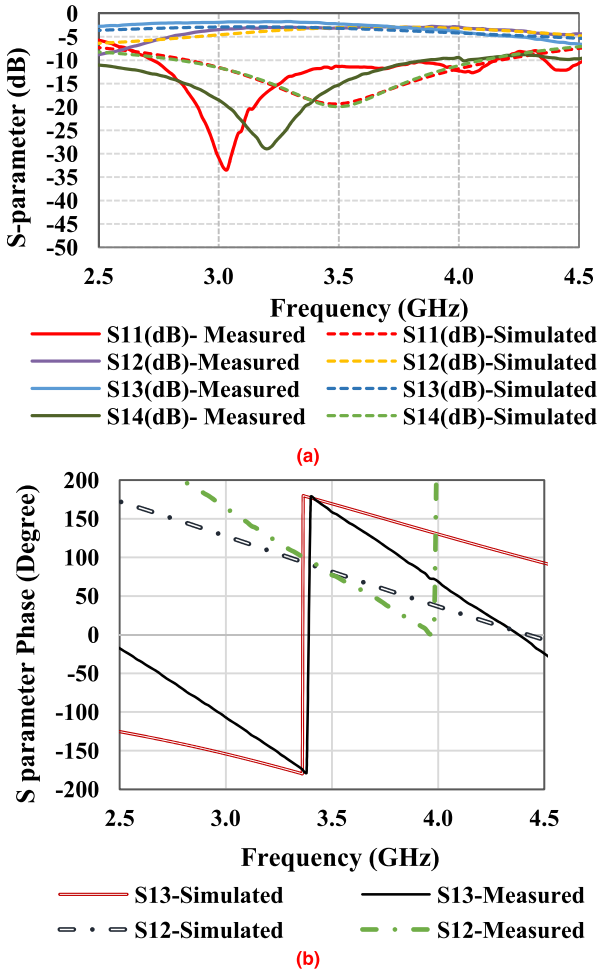

FIGURE 3. (a) S-Parameter response of the proposed simulated and fabricated BLC (b) Phase difference between the proposed simulated and fabricated prototype of the BLC.

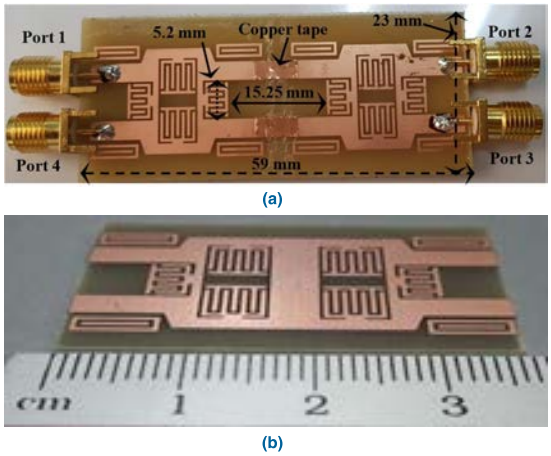

FIGURE 4. (a) Fabricated prototype of the 0dB crossover by cascading two 3dB BLC using FR4 substrate and copper tape, (b) Fabricated prototype of the compact 0dB crossover two 3dB BLC using FR4 substrate.

are same, so the compact designed crossover is selected for the development of the BM. The simulated and measured insertion loss is -0.19 dB and -0.5dB, respectively, at the operating frequency of 3.5GHz. Similarly, the simulated and

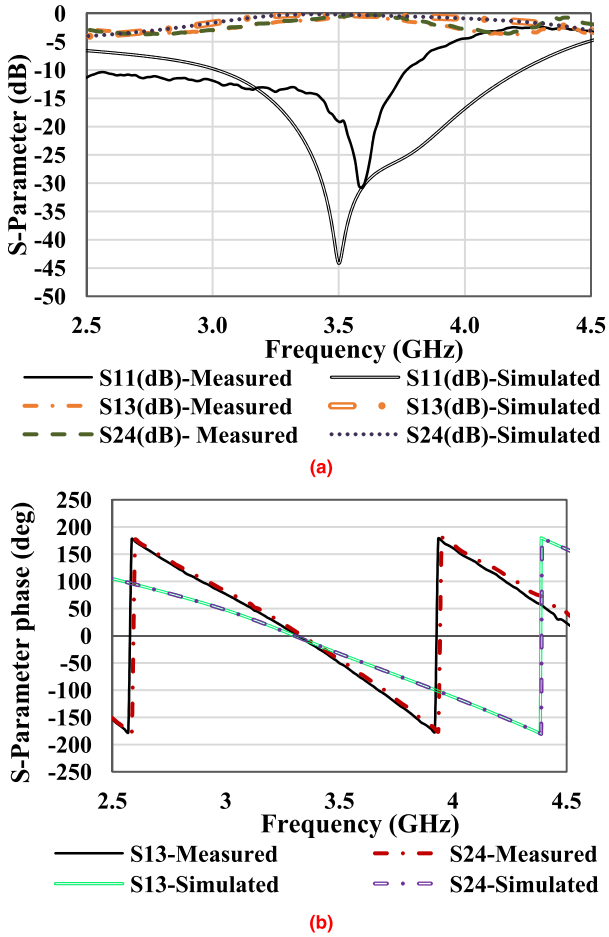

FIGURE 5. (a) S-Parameter response of the proposed simulated and fabricated compact 0dB crossover (b) Phase difference between the proposed simulated and fabricated prototype of the compact 0dB crossover.

measured phase difference between S_{31} and S_{24} is 0°, and 5°, respectively, which mean the phase shift introduced is very small and close to 0°. Fig. 5(a) shows the S-parameter response of simulated and measured compact 0dB crossover, whereas Fig. 5(b) shows the simulated and measured phase difference between S_{31} and S_{24}, respectively. The measured insertion loss and the phase difference validated the design specification mentioned in Table 2.

C. 4 × 4 BUTLER MATRIX PERFORMANCE

The planar single layer implementation of the 4 × 4 compact BM with improved bandwidth is performed by the combination of above designed 3dB BLC using open coupled lines and IDC-CRLH TL, 0dB crossover and 45° phase shifter at the centre frequency of 3.5GHz. As shown in Fig. 6(a), we have used the RF coaxial cables of 20 cm to develop the 45° phase shift, SMA L-shaped male-female RF jacks and, SMA male-female RF connectors to make the connection between the coupler and the crossover. Fig. 6(a) shows the hybrid implementation of the 4 × 4 BM which is good for the proof-of-concept but cannot be implemented as the BFN in 5G antenna array systems because of size constraints and

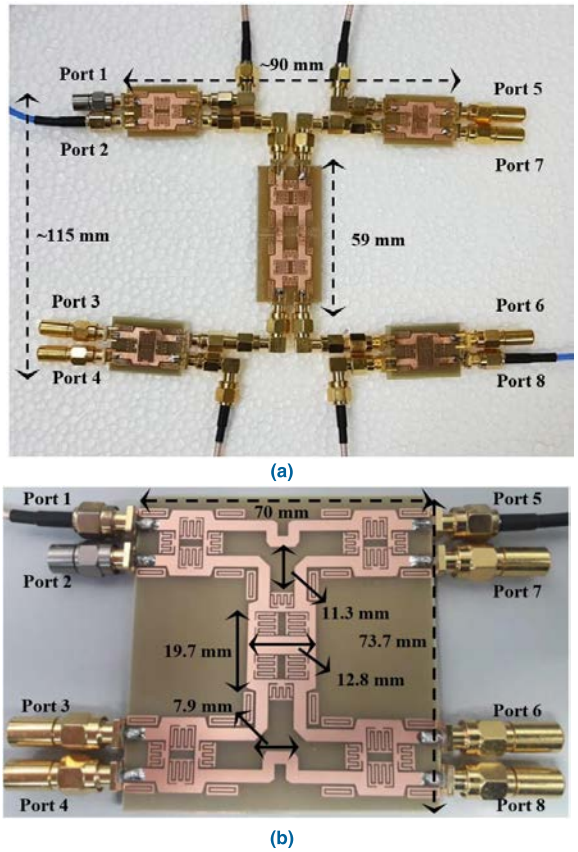

FIGURE 6. (a) Hybrid 4×4 BM by using the combination of BLCs and Crossovers with the help of SMA male-female RF connectors, SMA L-shape male-female RF jacks and RF coaxial cables (b) Compact 4×4 BM fabricated on a single FR4 substrate.

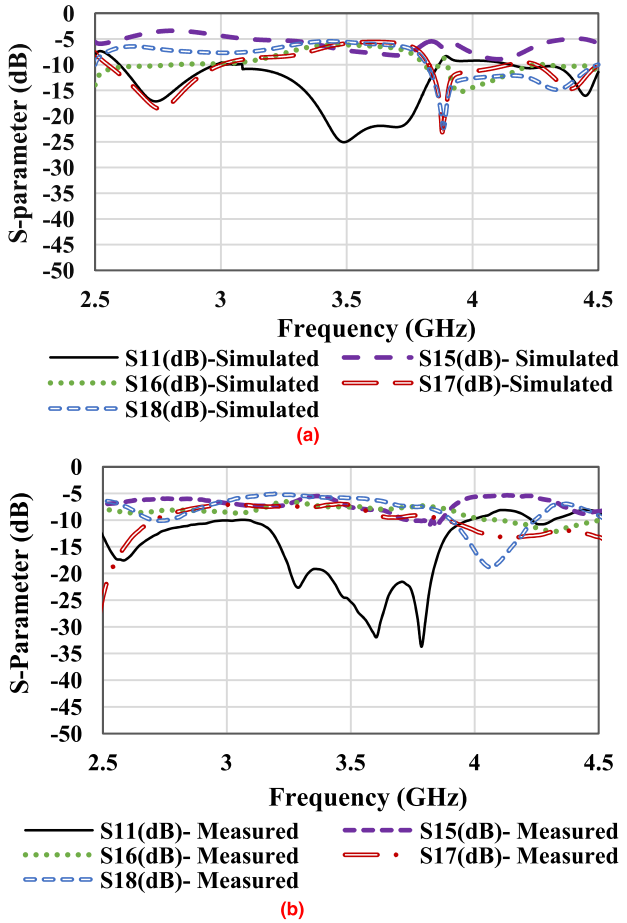

FIGURE 7. Shows the (a) Simulated and (b) Measured response of the insertion loss and return loss for port 1 excitation, respectively.

the extra losses induced by the SMA transitions and coaxial cables. In order to make the design compact and realistic for the implementation in 5G antenna array systems, it is fabricated by combining all the components on a single FR4 PCB sharing a common ground plane, as shown in Fig. 6(b). The compact design has a total area of 70mm × 73.7mm, as shown in Fig. 6(b). The simulated and measured results from both the 4 × 4 BM structures presented in Fig. 6(a-b) shows a good match, although there were some variations observed in the results which could be due to the extra losses and phase shifts induced by the cables and connectors. So, the discussion related to the results from now onwards will be based on the compact structure of the BM as shown in Fig. 6(b).

Fig. 6(b) shows the configuration of 4 × 4 BM, when a signal given to the input ports (port 1, port 2, port 3, port 4) is transferred to the output ports (port 5, port 6, port 7, port 8) with equal amplitude and specified phase difference as mentioned in Table 1.

Fig. 7(a-b) shows the simulated and measured results of the insertion and return losses, respectively when port 1 is excited, and all the other ports are terminated with 50Ω loads. These results show that the measured and simulated range of return loss is better than 13 dB and insertion loss detected at port 5, port 6, port 7 and port 8 is -7 ± 2dB from 3.2 GHz to 3.8GHz, respectively. So, the power splitting among the four output ports is approximately equal as per the insertion loss result. The measured return loss is −25dB and the average insertion loss (S_{15}, S_{16}, S_{17}, S_{18}) is −7dB at the operating frequency of 3.5GHz. The results obtained from the below graph validated our design specification mentioned in Table 2 are very promising and can be used in upcoming 5G systems.

Fig. 8(a-b) illustrates a good agreement between the simulated and measured results of the phase shift of adjacent output ports, when port 1 is excited. The phase difference between adjacent ports should be −45° as per the design consideration in Table 1. In the simulation, phase difference was −44.2° between port 5 and port 6 ($S_{16} - S_{15}$), −52.8°between ports 6 and port (S_{17}-S_{16}) and -40.3° between ports 7 and port 8 (S_{18}-S_{17}), respectively. So, the errors were 0.8, 7.8 and 4.7 degrees introducing an average error of 4.4 degrees, respectively. In the measured results, the phase difference was −42.7° between port 5 and port 6 (S_{16}-S_{15}), −51.4° between ports 6 and port 7 ($S_{17} - S_{16}$) and −54° between ports 7 and port 8 ($S_{18} - S_{17}$), respectively. So, the errors were 2.3, 6.4 and 9 degrees introducing an average error of 5.9 degrees. This small error in phase is due to the

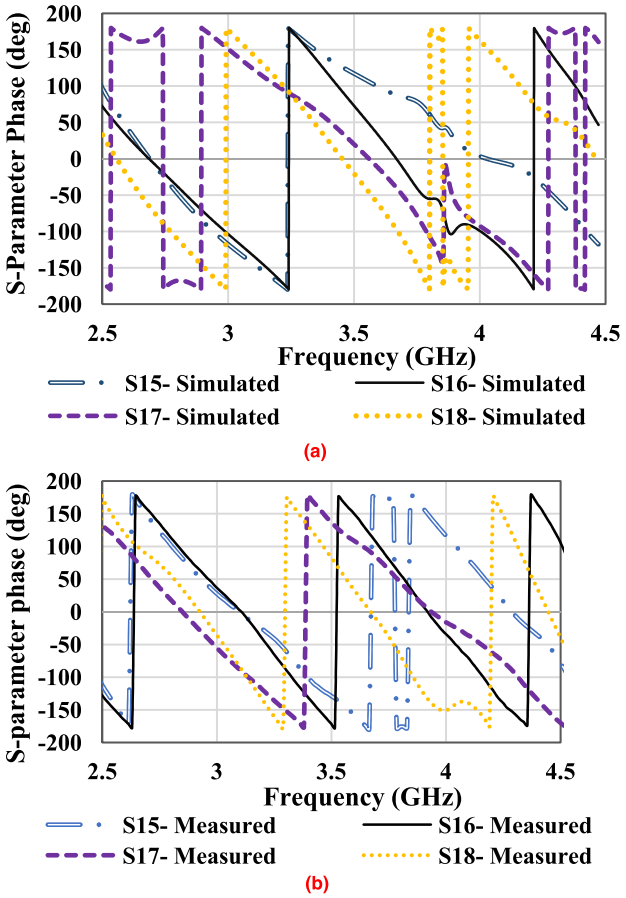

FIGURE 8. Shows the (a) Simulated and (b) Measured results of the phase shift of adjacent output ports, when Port 1 is excited.

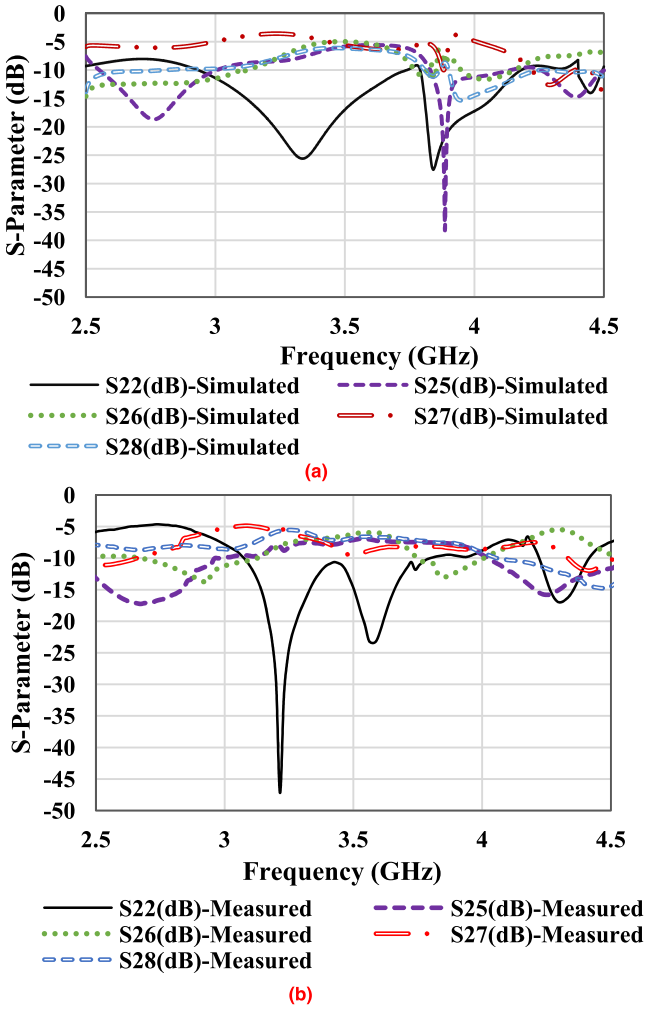

FIGURE 9. Shows the (a) Simulated and (b) Measured results of the insertion and return loss for the Port 2 excitation, respectively.

variation in the electrical permittivity parameter of the lossy FR4 substrate. This frequency shift problem can be solved in future by using a low-loss Rogers substrate. These results suggest a very good agreement between the simulated and the measured phase difference in value, although the quadrant is different, as mentioned in the below Table 3.

Fig. 9(a-b) show the simulated and measured results of the insertion and return loss, when port 2 is excited, and all other ports are terminated with 50Ω load. These results in Fig. 9 (a-b) show that the measured and simulated range of return loss is better than 14 dB and insertion loss detected at port 5, port 6, port 7 and port 8 is -7 ± 2dB from 3.2 GHz to 3.7GHz, respectively. So, the power splitting among the four output ports is approximately equal as per the insertion loss results. The measured return loss is -15dB and the average insertion loss (S_{25}, S_{26}, S_{27}, S_{28}) is -7dB at the operating frequency of 3.5GHz. The results in Fig. 9(a-b) are in agreement with each other when port 2 is excited, which suggest excellent BM performance.

Fig. 10(a-b) illustrates the results when port 2 is excited, and it shows a good agreement between the simulated and measured results of the phase shift of adjacent output ports. The phase difference between the adjacent ports should be 135° as per the design consideration provided in Table 1. In the simulation, it is found that the phase difference between the output ports is 145°, 129°, 141°, respectively at the center frequency. These values differ from the desired value of 135° by 10, 6 and 6 degrees introducing an average error of 7.3 degrees. In the measured results, the phase difference between output ports is 139°, 142°, 130.3°, respectively, at the centre frequency of 3.5GHz. So, the errors were 4, 7 and 4.7 degrees introducing an average error of 5.2 degrees and very good agreement between simulated and measured phase difference in value.

Fig. 11(a-b), shows the simulated and measured results of the insertion and return loss, when port 3 is excited, and all other ports are terminated with 50Ω load. These results in Fig. 11 (a-b) show that the measured and simulated range of return loss is better than 13 dB and the insertion loss detected at port 5, port 6, port 7 and port8 is -7 ± 2dB between 3.2 GHz to 3.75GHz frequency band. So, the power splitting among the four output ports is approximately equal as per the insertion loss results. The measured return loss is -17dB and the average insertion loss (S_{35}, S_{36}, S_{37}, S_{38}) is -7.7dB at the operating frequency of 3.5GHz. The result obtained from the

TABLE 3. Simulated and measured phase difference of the proposed butler matrix at 3.5 GHz.

Ports	Phase difference between Port 5 and Port 6 (Degrees)		Phase difference between Port 6 and Port 7 (Degrees)		Phase difference between Port 7 and Port 8 (Degrees)		Desired Phase Difference (Degrees)
	Simulated	Measured	Simulated	Measured	Simulated	Measured	
Port 1	-44.2	-42.7	-52.8	-51.4	-40.3	-54	-45
Port 2	145	139	129	142	141	130.3	135
Port 3	-141.6	-136.5	-128	-141	-146.5	146	-135
Port 4	42.6	47.4	51	44	50	46.8	45

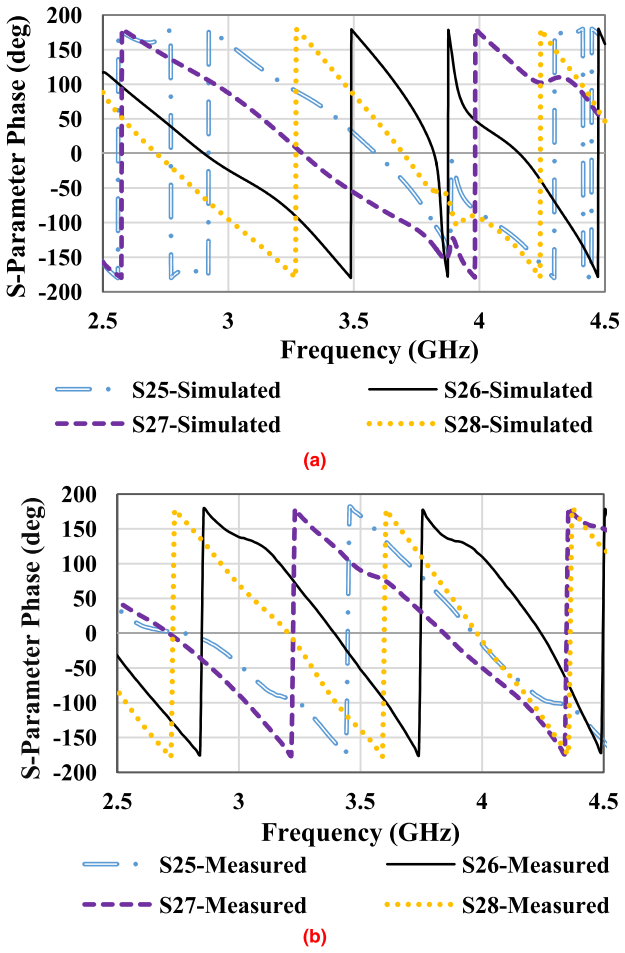

FIGURE 10. Shows the (a) Simulated and (b) Measured results of the phase shift of adjacent output ports, when Port 2 is excited.

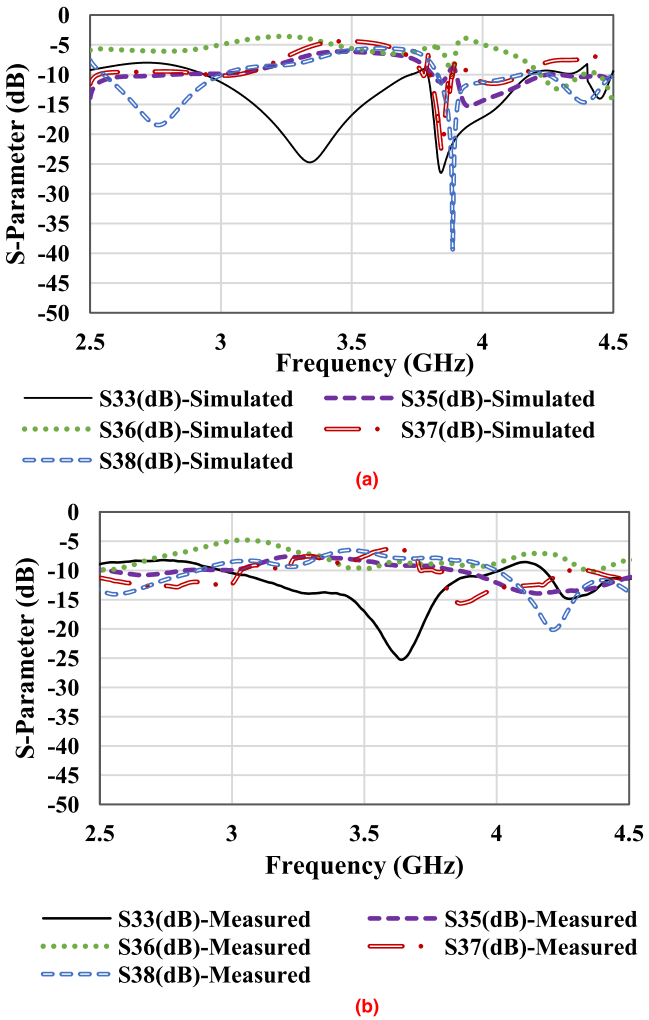

FIGURE 11. Shows the (a) Simulated and (b) Measured results of the insertion and return loss for Port 3 excitation, respectively.

below graph shows good agreement between simulated and measure results.

Fig. 12(a-b), illustrates a good agreement between the simulated and measured results of the phase shift of adjacent output ports, when port 3 is excited. The phase difference between the adjacent ports should be −135° as per the design consideration in Table 1. In the simulation results; the phase difference was −141.6° between port 5 and 6 (S_{36}-S_{35}), −128° between ports 6 and 7 (S_{37}-S_{36}) and −146.5° between ports 7 and 8 (S_{38} − S_{37}), respectively. So, the errors were 6.6, 7 and 11.5 degrees introducing an average error of 8.3 degrees, respectively. Whereas, in the measured results, the phase difference was −136.5° between port 5 and 6 (S_{36}-S_{35}), −141° between ports 6 and 7 (S_{37}-S_{36}) and −146° between ports 7 and 8 (S_{38}-S_{37}), respectively. So, the errors were

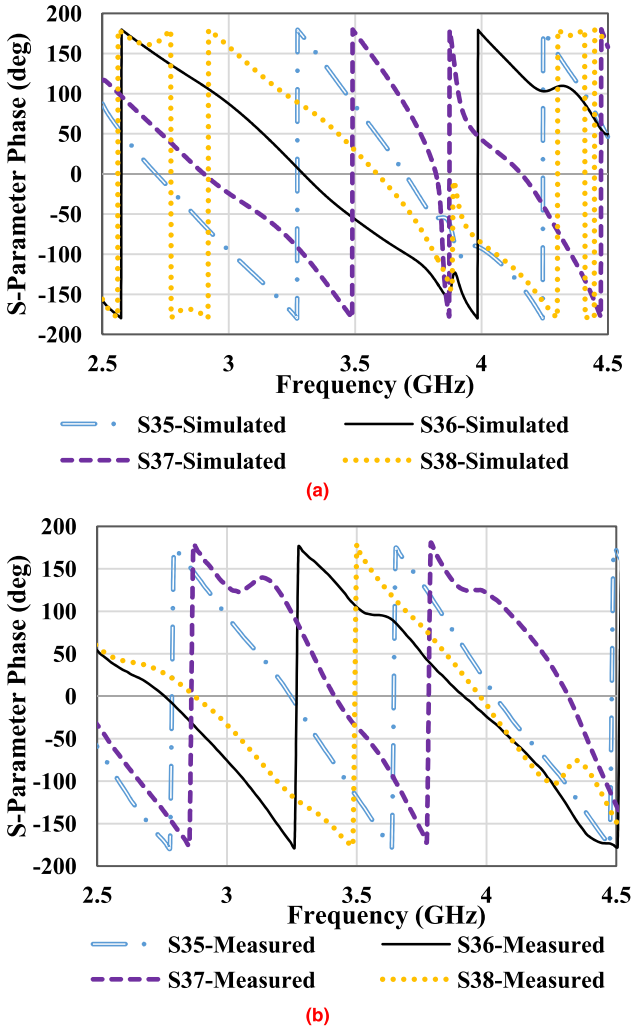

FIGURE 12. Shows the (a) Simulated and (b) Measured results of the phase shift of adjacent output ports, when Port 3 is excited.

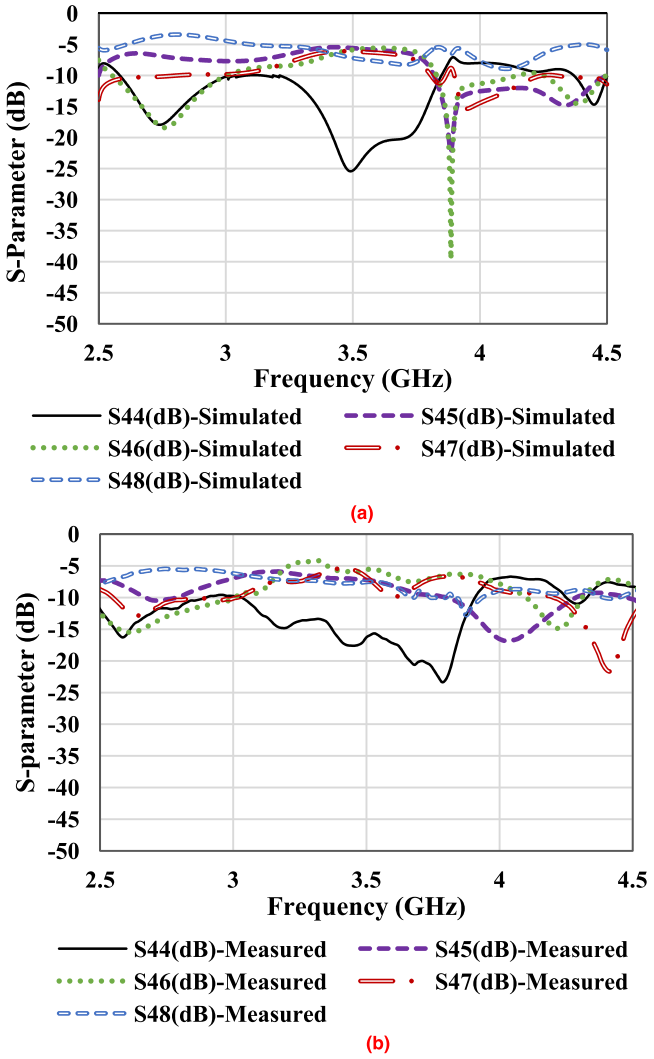

FIGURE 13. Shows the (a) Simulated and (b) Measured results of the insertion and return loss for Port 4 excitation.

1.5, 6 and 11 degrees, respectively introducing an average error of 6.1 degrees and very good agreement between the simulated and measured phase difference in value but the quadrant is different as summarized in Table 3.

Fig. 13(a-b) shows the simulated and measured insertion and the return loss results, when port 4 is excited, and all other ports are terminated with a 50Ω load. These results show that the measured and simulated range of return loss is better than 13 dB and insertion loss detected at port 5, port 6, port 7 and port 8 is -7 ± 2dB between the 3.2 GHz to 3.75GHz frequency band. So, the power splitting among the four output ports is approximately equal as per the insertion loss results shown in Fig 13 (a-b). The measured return loss is -16.3dB and the average insertion loss (S_{45}, S_{46}, S_{47}, S_{48}) is -6.75dB at the operating frequency of 3.5GHz.

Fig. 14(a-b) illustrates a good agreement between the simulated and measured results of the phase shift of adjacent output ports, when port 4 excited. The phase difference between the adjacent ports should be 45° as per the design consideration in summarized Table 1. In simulation results; it is found that the phase difference between the output ports is 42, 51°, 50° respectively at the centre frequency. These values differ from the desired value by 2.3, 6 and 5 degrees introducing an average error of 4.4 degrees. In the measured results, the phase difference between output ports is 47.4°, 44°, 46.8° respectively, at the centre frequency of 3.5GHz. So, the errors were 2.4, 1 and 1.8 degrees introducing an average error of 1.7 degrees and very good agreement between simulated and measured phase difference in value but the quadrant is different as summarized in Table 3.

Table 3 and Table 4 summarize the simulated and measured phase difference between the ports and the S-parameter of the proposed BM at the operating frequency of 3.5GHz, respectively. It can be seen from the Table 3 and Table 4 that at the 3.5GHz operating frequency, the phase difference between all the ports has a very good agreement with the desired value and the magnitude tolerance of ±2 dB.

TABLE 4. Simulated and measured s-parameter of the proposed butler matrix at 3.5 GHz.

Ports	Insertion Loss (dB) Port 5		Insertion Loss (dB) Port 6		Insertion Loss (dB) Port 7		Insertion Loss (dB) Port 8		Desired Value (dB)
	Simulated	Measured	Simulated	Measured	Simulated	Measured	Simulated	Measured	
Port 1	-7.2	-7.5	-6.1	-7.5	-5.85	-7.2	-5.6	-5.8	-7 ± 2
Port 2	-5.8	-7.1	-5	-6.2	-5.6	-8	-6.1	-6.8	-7 ± 2
Port 3	-6.1	-8.3	-5.6	-8.4	-5	-7.5	-5.85	-6.7	-7 ± 2
Port 4	-5.6	-7.2	5.9	-5.6	-6.1	-6.7	-7.2	-7.5	-7 ± 2

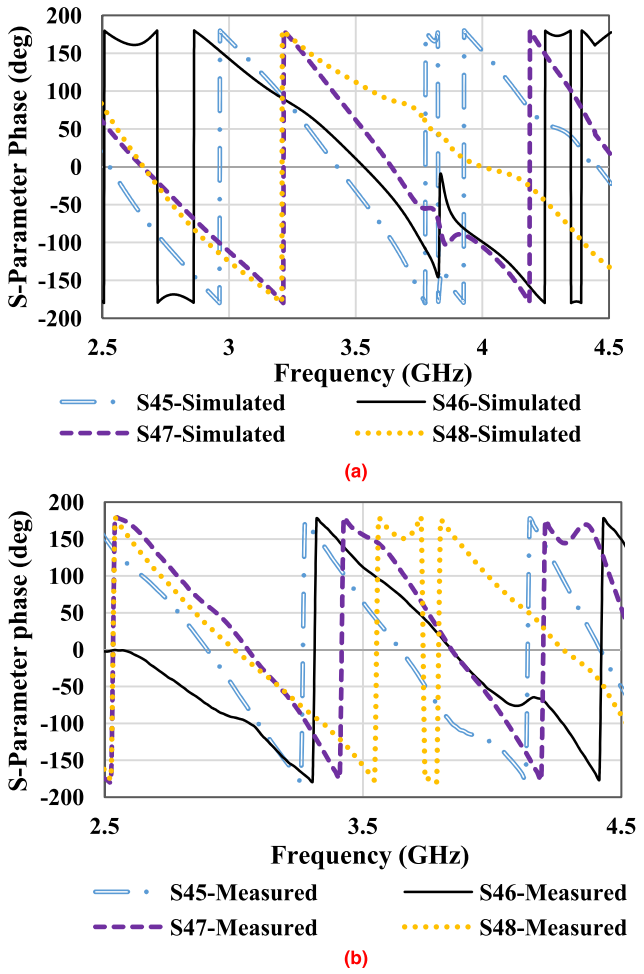

FIGURE 14. Shows the (a) Simulated and (b) Measured results of the phase shift of adjacent output ports, when Port 4 excited.

III. COMPARITIVE STUDY

A comparison of the proposed planar and compact BM with the existing works is shown in Table 5. The comparison table shows that our proposed BM has good improvement both in terms of bandwidth and size reduction which are major design consideration for the future 5G system deployments. The return loss, insertion loss and the phase difference for the proposed BM achieved design specification summarized in Table 1 and 2. The references cited in Table 5 were selected

TABLE 5. Performance of the proposed butler matrix at 3.5 GHz with existing planar technology based BM.

Reference / Year	Frequency f_o (GHz)	Bandwidth (MHz)	Size (cm)
[24] / 2011	1.8	200	11.9 ×10.9
[18] / 2014	0.86	150	10.9 × 8.93
[28] / 2016	2.4	300	15.4 × 11.7
[16] / 2017	2.5	200	11.5 × 6.4
[26] / 2017	2.5	400	12 ×15
[25] / 2018	6	2300	10 × 11
[27] / 2019	2.44	200	9.6 × 9.6
[12] / 2019	2.4	900	17 × 17
[This Work] / 2019	3.5	550	7 × 7.37

based on the planar single-layer BM and their respective operating frequency. From Table 5, it is very important to note that in most of the presented designs, the researchers are either trying to improve the bandwidth or reducing the size. Although, the work presented in this paper shows the improvement in the bandwidth and the size reduction at the same time.

IV. CONCLUSION

In this paper, a novel 4 × 4 butler matrix has been proposed, designed and fabricated for the 5G antenna array system. The proposed butler matrix is designed using the composite right/left handed transmission-line metamaterial structure, which is based on open-circuits coupled-lines and interdigital capacitors. The proposed butler matrix has the advantage of compact size (70mm × 73.7mm) and improved bandwidth (550MHz) as compared to the previous designs discussed in the literature and summarized in the previous section. Moreover, the circuit size has been reduced by 75%, and the overall bandwidth has been improved by 8.2 times more than the conventional butler matrix [29].

The proposed butler matrix is fabricated using two different techniques. The first one was the hybrid 4 × 4 butler matrix design by using the combination of BLCs, crossovers, SMA male-female RF connectors and the coaxial cables. The second 4 × 4 butler matrix design was fabricated on a

single FR4 substrate in which the BLCs, crossovers and phase shifters are sharing the common ground plane which leads to a compact structure with improved bandwidth. The simulated and measured return loss, insertion loss and phase difference between the ports shows good correlation with the design specification summarized in Table 2. The measured phase difference between the output ports are −45°,135°, −135° and +45°, respectively achieved with a maximum average phase tolerance of 5° at 3.5GHz based on the excitation of the input port, so it is possible to switch in a different direction at the same time. Based on the results, the proposed butler matrix design is considered to be a suitable candidate for the beamforming network in 5G antenna array systems.

ACKNOWLEDGMENT

The authors would like to acknowledge all members of the Advanced RF and Microwave Research Group (ARFMRG).

REFERENCES

[1] J. G. Andrews, "What will 5G be?" *IEEE J. Sel. Areas Commun.*, vol. 32, no. 6, pp. 1065–1082, Jun. 2014.
[2] T. S. Rappaport, S. Sun, R. Mayzus, H. Zhao, Y. Azar, K. Wang, G. N. Wong, J. K. Schulz, M. Samimi, and F. Gutierrez, "Millimeter wave mobile communications for 5G cellular: It will work!" *IEEE Access*, vol. 1, pp. 335–349, 2013.
[3] D. Muirhead, M. A. Imran, and K. Arshad, "A survey of the challenges, opportunities and use of multiple antennas in current and future 5G small cell base stations," *IEEE Access*, vol. 4, pp. 2952–2964, 2016.
[4] M. Agiwal, A. Roy, and N. Saxena, "Next generation 5G wireless networks: A comprehensive survey," *IEEE Commun. Surveys Tuts.*, vol. 18, no. 3, pp. 1617–1655, 3rd Quart., 2016.
[5] T. S. Rappaport, Y. Xing, O. Kanhere, S. Ju, A. Madanayake, S. Mandal, A. Alkhateeb, and G. C. Trichopoulos, "Wireless communications and applications above 100 GHz: Opportunities and challenges for 6G and beyond," *IEEE Access*, vol. 7, pp. 78729–78757, 2019.
[6] A. Costanzo and D. Masotti, "Energizing 5G: Near- and far-field wireless energy and data trantransfer as an enabling technology for the 5G IoT," *IEEE Microw.*, vol. 18, no. 3, pp. 125–136, May 2017.
[7] A. K. Pandey, "Design of a compact high power phased array for 5G FD-MIMO system at 29 GHz," in *Proc. Asia–Pacific Microw. Conf. (APMC)*, New Delhi, India, Dec. 2016, pp. 1–4.
[8] J.-H. Kim, J.-H. Han, J.-S. Park, and J.-G. Kim, "Design of phased array antenna for 5G mm-wave beamforming system," in *Proc. IEEE 5th Asia–Pacific Conf. Antennas Propag. (APCAP)*, Kaohsiung, Taiwan, Jul. 2016, pp. 201–202, 26-29.
[9] I. Sfar, L. Osman, and A. Gharsallah, "Design of a 4 × 4 butler matrix for beamforming antenna applications," in *Proc. Medit. Microw. Symp. (MMS)*, 2014, pp. 1–4.
[10] W. Nie, Y. Fan, S. Luo, and Y. Guo, "A switched-beam microstrip antenna array with miniaturized butler matrix network," *Microw. Opt. Technol. Lett.*, vol. 57, no. 4, pp. 841–845, Apr. 2015.
[11] Y.-L. Li, Q. S. Liu, S. Sun, and S. S. Gao, "A miniaturised butler matrix based on patch hybrid couplers with cross slots," in *Proc. IEEE Antennas Propag. Soc. Int. Symp. (APSURSI)*, Orlando, FL, USA, Jul. 2013, pp. 2145–2146.
[12] K. T. Chandrasekaran, N. Nasimuddin, A. Alphones, and M. F. Karim, "Compact circularly polarized beam-switching wireless power transfer system for ambient energy harvesting applications," *Int. J. RF Microw. Comput.-Aided Eng.*, vol. 29, no. 1, p. e21642, 2019.
[13] P. Mariadoss, M. Rahim, and M. Aziz, "Design and implementation of a compact butler matrix using mitered bends," in *Proc. Asia–Pacific Microw. Conf. Proc.*, Suzhou, China, vol. 5, Mar. 2006, p. 4.
[14] A. Darvazehban, O. Manoochehri, M. A. Salari, P. Dehkhoda, and A. Tavakoli, "Ultra-wideband scanning antenna array with Rotman lens," *IEEE Trans. Microw. Theory Techn.*, vol. 65, no. 9, pp. 3435–3442, Sep. 2017.
[15] M. W. Sabri, N. A. Murad, and M. K. A. Rahim, "Wideband branch line coupler with open circuit coupled lines," *Int. J. Electr. Comput. Eng.*, vol. 7, no. 2, pp. 888–893, Apr. 2017.
[16] P. Bhowmik and T. Moyra, "Modelling and validation of a compact planar butler matrix by removing crossover," *Wireless Pers. Commun.*, vol. 95, no. 4, pp. 5121–5132, Aug. 2017.
[17] G. Tian, J.-P. Yang, and W. Wu, "A novel compact butler matrix without phase shifter," *IEEE Microw. Wireless Compon. Lett.*, vol. 24, no. 5, pp. 306–308, May 2014.
[18] M. Du and H. Peng, "Ultra-compact electromagnetic metamaterial transmission line and its application in miniaturized butler matrix," *Prog. Electromagn. Res. C*, vol. 55, pp. 187–197, Jan. 2014.
[19] *FR4 Material Datasheet*. Accessed: Oct. 21, 2018. [Online]. Available: https://www.oneseine.com/PCB-Datasheet-download_3.html
[20] D. M. Pozar, *Microwave Engineering*, 3rd ed. Hoboken, NJ, USA: Wiley, 2005.
[21] E. H. Fooks, *Microwave Engineering Using Microstrip Circuits*. New York, NY, USA: Prentice-Hall, 1990.
[22] C. Caloz and T. Itoh, *Electromagnetic Metamaterials: Transmission Line Theory and Microwave Applications*. Hoboken, NJ, USA: Wiley, 2005.
[23] R. Siragusa, H. V. Nguyen, P. Lemaître-Auger, S. Tedjini, and C. Caloz, "Modeling and synthesis of the interdigital/stub composite right/left-handed artificial transmission line," *Int. J. RF Microw. Comput.-Aided Eng.*, vol. 19, no. 5, pp. 549–560, Sep. 2009.
[24] H.-X. Xu, G.-M. Wang, and X. Wang, "Compact butler matrix using composite right/left handed transmission line," *Electron. Lett.*, vol. 47, no. 19, p. 1081, 2011.
[25] R. K. M. Lou, M. Naser-Moghadasi, and R. A. Sadeghzadeh, "Broadband planar aperture-coupled antenna array for WLAN and ITS beam-steering applications," *Radio Sci.*, vol. 53, no. 2, pp. 200–209, Feb. 2018.
[26] S. Kuwana, H. Hayashi, and R. Ueda, "Simple design of four-element planar butler matrix using two-section branch-line hybrids," *IEEJ Trans. Elect. Electron. Eng.*, vol. 12, pp. S187–S188, Jun. 2017.
[27] G. A. Adamidis, I. O. Vardiambasis, M. P. Ioannidou, and T. N. Kapetanakis, "Design and implementation of single-layer 4 × 4 and 8 × 8 butler matrices for multibeam antenna arrays," *Int. J. Antennas Propag.*, vol. 2019, pp. 1–12, Mar. 2019, doi: 10.1155/2019/1645281.
[28] O. A. Safia, M. Nedil, M. C. E. Yagoub, and W. Yusuf, "Optically transparent compact 4×4 butler matrix for Wi-Fi applications," *Prog. Electromagn. Res.*, vol. 58, pp. 119–124, Jan. 2016.
[29] N. V. Priyadarshan and A. Thenmozhi, "Beam forming network using 4 × 4 narrowband butler matrix for tracking and localization applications," in *Proc. Int. Conf. Intell. Comput. Control Syst. (ICICCS)*, Jun. 2017, pp. 1241–1246.

ARSHAD KARIMBU VALLAPPIL received the B.Tech. degree in electronics and communication engineering from the University of Calicut, Kerala, India, in 2009, and the M.Tech. degree in electronics engineering from Pondicherry University, Puducherry, India, in 2013. He is currently pursuing the Ph.D. degree in electrical engineering from the University Teknologi Malaysia, Malaysia. His research interests are RF and microwave systems, antenna arrays, and beamforming networks.

MOHAMAD KAMAL A. RAHIM (Senior Member, IEEE) was born in Alor Setar, Kedah, Malaysia, in 1964. He received the B.Eng. degree in electrical and electronic engineering from the University of Strathclyde, U.K., in 1987, the master's degree in engineering from the University of New South Wales, Australia, in 1992, and the Ph.D. degree in the field of wideband active antenna from the University of Birmingham, U.K., in 2003. From 1992 to 1999, he was a Lecturer with the Faculty of Electrical Engineering, Universiti Teknologi Malaysia, where he was a Senior Lecturer with the Department of Communication Engineering, from 2005 to 2007. He is currently a Professor with the Universiti Teknologi Malaysia. His research interests include the design of active and passive antennas, dielectric resonator antennas, microstrip antennas, reflectarray antennas, electromagnetic bandgap, artificial magnetic conductors, left-handed metamaterials, and computer-aided design for antennas.

BILAL A. KHAWAJA (Senior Member, IEEE) received the B.S. degree in computer engineering from the Sir Syed University of Engineering and Technology, Karachi, Pakistan, in 2002, the M.Sc. degree in communication engineering and signal processing from the University of Plymouth, Plymouth, U.K., in 2005, and the Ph.D. degree in electrical engineering from the University of Bristol, Bristol, U.K., in 2010. From 2003 to 2004, he was a Software Engineer with Simcon International Pvt., Ltd., Pakistan. From 2010 to 2016, he was an Assistant Professor with the Electronics and Power Engineering Department, PN-Engineering College, National University of Science and Technology (NUST), Karachi. In 2015, he was a Visiting Postdoctoral Researcher with the Lightwave Systems Research Laboratory, Queens University, Kingston, Canada, where he was involved in the Natural Sciences and Engineering Research Council (NSERC), Canada, and the CREATE Next-Generation Optical Network (NGON) Project on the characterization and measurements of 25GHz RF signal generation optical comb sources. He is currently an Associate Professor with the Department of Electrical Engineering, Faculty of Engineering, Islamic University of Madina, Madina, Saudi Arabia. He has authored or coauthored several journals and IEEE proceeding publications. His current research interests include next-generation of millimetre-wave (mm-wave) radio-over-fiber and optical communication systems, mm-wave and THz signal generation mode-locked lasers and RF transceiver design and antennas design/characterization for the Wi-Fi/IoT/UAVs/FANETs/5G systems/UWB wireless body area networks, wireless sensor networks, and millimeter-wave frequency bands. He is an Active Reviewer for many reputed IEEE journals and letters.

MUHAMMAD NAEEM IQBAL was born in Mangla, Pakistan, in 1987. He received the bachelor's and master's degrees in electrical engineering from the National University of Sciences and Technology, Pakistan, in 2009 and 2013, respectively. He is currently pursuing the Ph.D. degree in electrical engineering with the Universiti Teknologi Malaysia. His research interests include the transmitarray antennas, reflectarray antennas, beam forming, and polarization converters.